

# Synthesis of carbon nanotubes in stagnation-point liquid-pool flames

Hu, Wei-Chieh<sup>1</sup>, Hou, Shuhn-Shyurng<sup>2</sup>, Lin, Ta-Hui<sup>1</sup>

<sup>1</sup>Department of Mechanical Engineering, National Cheng Kung University  
Tainan 70101, Taiwan, Republic of China

<sup>2</sup>Department of Mechanical Engineering, Kun Shan University  
Tainan 71003, Taiwan, Republic of China

## 1 Introduction

Recently, carbon nanostructures have drawn much attention due to their unique mechanical, electrical, and chemical properties. Great efforts have been devoted to the synthesis of carbon nanostructures, such as C<sub>60</sub> (buckminsterfullerene) [1], carbon nanotubes (CNT) [2], graphene [3] and other nanostructures. Different methods are employed for synthesis of carbon nanostructures such as arc discharge, laser ablation, and chemical vapor deposition. In addition, flame has been applied in synthesizing a great variety of nanostructures [4-6]. Compared with other methods, flame synthesis is more economical due to simple equipment and low energy consumption. In flame synthesis, fuels and catalysts are the major parameters. Though other factors such as combustion modes (diffusion flames or premixed flames), configurations (co-flow or counterflow), and oxygen concentration can also affect flame characteristics. The selection of fuel dictates flame temperature and species of radicals which are critical to the synthesis of nanostructures.

Most researches employed gaseous fuel for synthesis of carbon nanostructures, like methane [4], ethylene and acetylene [5]. Only few researches applied liquid fuel flames in synthesis of carbon nanostructures. Liu et al. [7] employed a common laboratory ethanol burner and two different catalysts in the study. They synthesized CNTs and carbon nanofibers (CNFs) with Type 304 austenitic stainless steel and low carbon mild steel as catalyst, respectively. With the observation from scanning electron microscope (SEM), transmission electron microscope (TEM), and Raman spectra, the authors concluded that the CNTs grown on stainless steel substrates possess higher graphitic degree of order than the CNFs on mild steel substrates during ethanol flaming synthesis. Hall et al. [8] applied premixed flames to analyze the influence of fuel structure on the synthesis of carbon nanostructure. Three hydrocarbon fuel feedstocks of different chemical structures (ethylene, ethyl benzene and ethyl alcohol) were employed. Fuels were mixed with air to form premixed, laminar fuel-rich flames with various equivalence ratios, and liquid fuels (ethanol, ethyl benzene) went through pre-vaporization before mixing. CNTs and CNFs of varying diameters and lengths were synthesized. They found that only ethylene and ethanol generated tubular carbon nanostructures, and the concentrations of aliphatic species had linear correlations with the mean diameter of the nanostructures. However, there is still a lack of understanding about using high C-H ratio, and long chained hydrocarbons as fuels for the synthesis of carbon nanostructures.

The oxygen concentration strongly influenced flame characteristics (such as the formation of soot layer, flame extinction, flame position, radical and temperature distributions) and in turn synthesis results. Radical concentrations (carbon source) and temperature (heat source) are two important factors for the synthesis of carbon nanostructures. Both of them will be influenced by the oxygen concentration, exit velocity and sampling position. Additionally, suitable deposition time is required for the growth of nanostructures. In view of the research in need, we put particular focus on the influence of liquid fuel and oxygen concentration on the fabrication of carbon nanostructures using n-heptane diffusion flames in a stagnation-point flow and a catalytic Ni substrate.

## 2 Experimental setup

A stagnation-point liquid-pool system [9] was employed in this study (Fig. 1). A liquid pool supplied with fuel from the indicator, and the upper burner impinged gaseous mixture of nitrogen (purity 99.5%) and oxygen (purity 99.5%) with uniform injection velocity onto the liquid pool which formed a stagnation-point flow. The upper burner and the liquid pool were vertically aligned, and had identical diameters of 50 mm with separation distance of 20 mm. The height of liquid in the pool remained constant by continuously liquid supplied from the indicator during the experiment. A water cooling system was set around the liquid pool to prevent overheating and an exhaust system was set to remove combustion products. The gas volume flow rates were controlled by separate rotameters and the exit velocity ( $V$ ) of the upper burner was varied. The volume percentage of oxygen is denoted by  $\Omega_{\text{O}}$ . In the experiments, n-heptane was employed as fuel and pure nickel grids were employed for collecting combustion products. The grid is 3 mm in diameter and 0.2 mm in thickness of 200 meshes. The grids without pretreatment acted as the catalytic substrate and no other catalysts were added. The deposition time was 120 s. The gas temperature was measured by an R-type thermocouple (Pt/Pt-13% Rh). Field emission scanning electron microscopy (FE-SEM, JEOL JSM-7000F, operated at an accelerating voltage of 20 kV) was employed to characterize the deposited materials.

## 3 Results and discussion

The combustion characteristics of the diffusion flame in the liquid pool system were examined before the synthesis of carbon nanostructures. Fig. 2 indicates a part of direct photographs of the n-heptane flame under different  $\Omega_{\text{O}}$  and  $V$  ( $\Omega_{\text{O}}$  up to 21%). In the experiments,  $\Omega_{\text{O}}$  varied from 12% to 40% and  $V$  varied from 20 to 40 cm/s. The variations of these two parameters strongly affected the position of blue flame and the formation of soot layer. In Fig. 2, blight yellow n-heptane flames with thick soot layers were observed at  $\Omega_{\text{O}} = 21\%$  and  $V = 20 - 40$  cm/s. As  $\Omega_{\text{O}}$  decreased from 21% to 17% - 19%, flames moved toward the pool. Meanwhile, the soot layers gradually became thinner and finally disappeared. While  $\Omega_{\text{O}}$  kept decreasing, the blue flames also became weaker and extinguished at  $\Omega_{\text{O}} = 11\% - 13\%$  depending on the exit velocities. The exit velocities affected flame heights directly. The heights of both blue flame and soot layer decreased and the flame was flattened.

The positions of blue flame fronts and soot layers were obtained from flame photographs by image analysis software. Fig. 3 shows the upper edges of blue flames and soot layers under different  $\Omega_{\text{O}}$  and  $V$ , and the z-axis is defined that  $z = 0$  mm at the liquid surface. As aforementioned, the heights of blue flame and soot layer decreased with the decrease of  $\Omega_{\text{O}}$  and the increase of exit velocity. However, the flame heights did not decrease linearly with the increase of exit velocities. At higher exit velocities ( $V = 30-40$  cm/s), less decrease of flame heights was found. As the exit velocity was increased, the flame was forced downward and the high temperature region moved closer to the liquid pool. It caused the vaporization rate of n-heptane to increase and balanced with gas flow from the upper burner. It is noteworthy that soot layers may have a supporting effect on the blue flames when the blue flames were lower than 4 mm. Once the soot layers were disappeared, the heights of blue flames dropped steeply from 4 to 3 mm.

Temperature is an important parameter of synthesizing carbon nanostructures. Fig. 4 shows the temperature distribution of heptane flames at different  $\Omega_O$ . Temperature decreased with  $\Omega_O$  under constant exit velocity. Vapor of heptane was heated by flame and the temperature gradually increased to the maximum at the position of blue flame around 4 mm above the liquid surface. At  $\Omega_O = 21\%$ , the maximum temperature may reach 1260°C. As  $\Omega_O$  decreased to 19%, 17% and 15%, the maximum temperature dropped to 1000°C, 930°C and 730°C, respectively. At  $\Omega_O = 13\%$ , the flame was near extinction, and the temperature only reached 630°C. The temperature distribution varied with the flame position due to the characteristics of diffusion flame. Thus, the sampling position of synthesis was defined by the distance apart from the blue flame.

Fig. 5 shows the SEM images of synthesized products. The sampling position was 1.5 mm below the blue flame. Figs. 5a to 5d indicate the synthesized results of  $\Omega_O = 21\%$  to 15%, respectively. As can be seen in Fig. 5a, no nanostructure was observed at  $\Omega_O = 21\%$ . The surface of grid was roughened under high temperature. At  $\Omega_O = 19\%$  (Fig. 5b), carbon nano-onions (CNOs) were found. CNOs are spherical structures with graphitic layers. In our experiments, diameters of CNOs ranged from 40 to 70 nm, and CNOs aggregated to form grape-like structures. As  $\Omega_O$  decreased to 17% (Fig. 5c), the yield of CNO dramatically decreased and only a small amount of CNOs remained. As  $\Omega_O$  kept decreasing, no CNOs but CNTs were found at  $\Omega_O = 15\%$  (Fig. 5d). The temperatures at the sampling positions of  $\Omega_O = 21\%$ , 19%, 17% and 15% were approximately 1250°C, 940°C, 870°C and 725°C, respectively. The absence of nanostructures at  $\Omega_O = 21\%$  may be caused by the high temperature. However, no CNTs were found at  $\Omega_O = 17\%$  at which the temperature was 870°C. Common synthesis temperature of CNTs by CVD is around 800°C. The growth of CNTs at  $\Omega_O = 15\%$  suggests that lower temperature (725°C) was required in heptane flame. The products varied from CNOs to CNTs while lowering  $\Omega_O$  from 19% to 15% with temperature difference of 215°C. It suggests that the ambient oxygen concentration can be considered as a controlling factor of synthesizing carbon nanostructures.

## 4 Conclusions

Carbon nanotubes were synthesized by n-heptane diffusion flames in a stagnation-point liquid pool system. Both the ambient oxygen concentration and exit velocity had significant influence on the flame synthesis of CNTs. Oxygen concentrations dominated the formation of soot layer, flame extinction, and flame heights. Additionally, the exit velocities also affected the flames. Higher exit velocities may lead to disappearance of soot layers, flame extinction at higher oxygen concentrations, and lower flame height. No nanostructures were found at  $\Omega_O = 21\%$ , and its corresponding temperature at the sampling position was 1250°C. CNOs and CNTs were synthesized at  $\Omega_O = 17\%$  and 15%, respectively. And their corresponding temperatures at the sampling positions were 870°C and 725°C. The temperature for synthesis of CNTs was lower than common synthesis temperature of 800°C using CVD. Compared with CNOs, CNTs tend to form at lower temperature and oxygen concentration in liquid pool stagnation flames.

## Acknowledgment

This work was supported by the National Science Council, Taiwan, ROC, under contract NSC99-2212-E-006-081-MY3.

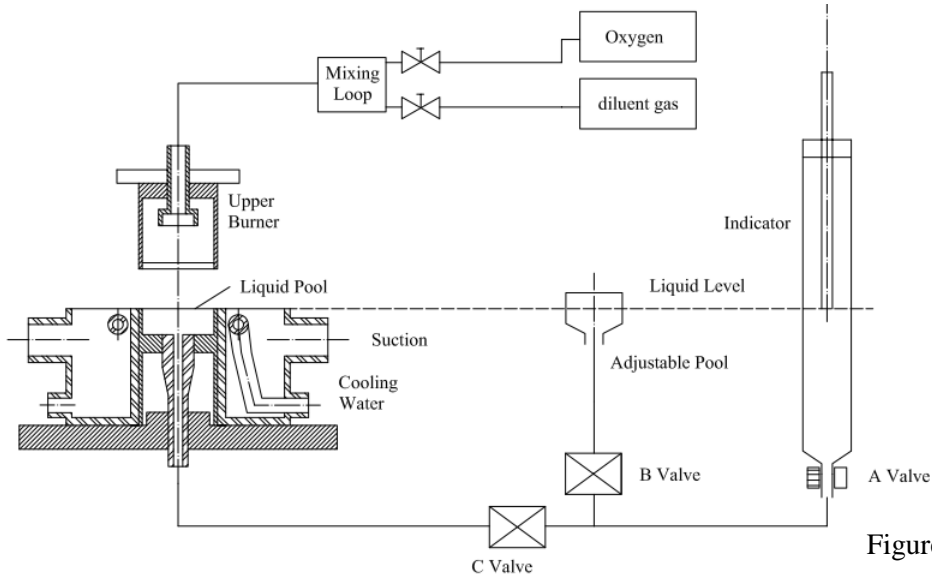


Figure 1. Experimental setup

		Heptane					
		$\Omega_o$					
V		12%	13%	15%	17%	19%	21%
20	cm/s						
25	cm/s						
30	cm/s						
35	cm/s						
40	cm/s						

Figure 2. Direct flame photographs of n-heptane pool in a stagnation-point flow for various injection velocities ( $V = 20-40$  cm/s) and oxygen concentrations ( $\Omega_o = 12\%-21\%$ ).

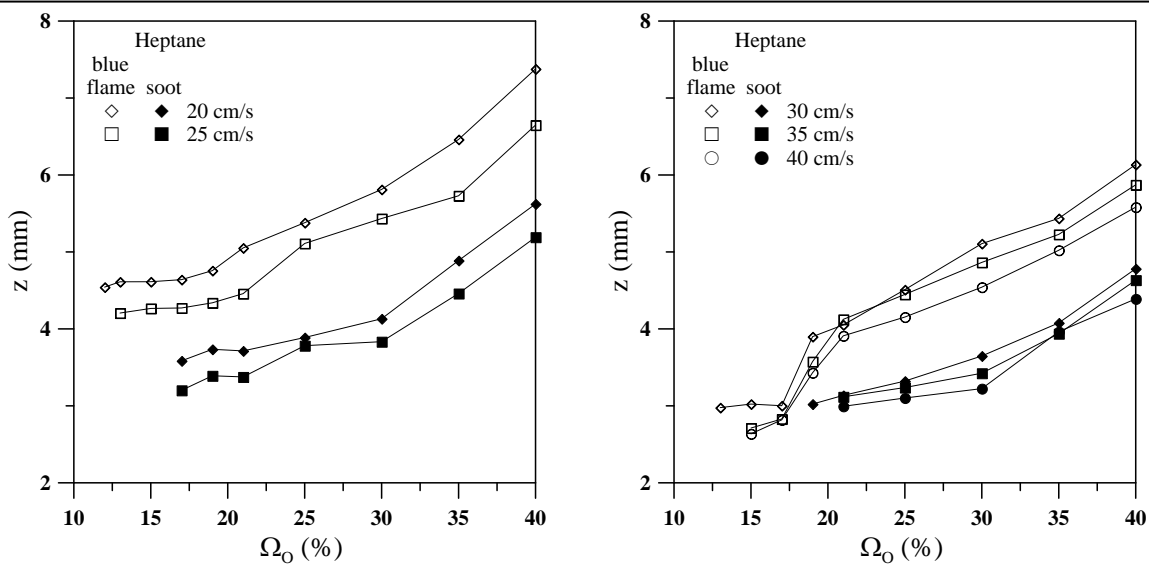


Figure 3. Measured heights of blue flame fronts and soot layers for  $\Omega_O = 12\%$ - $40\%$ . Left:  $V = 20$ - $25$  cm/s. Right:  $V = 30$ - $40$  cm/s.

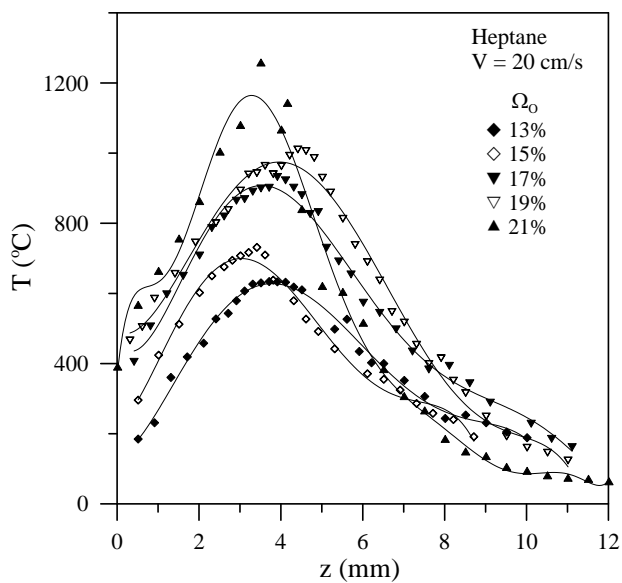


Figure 4. Axial temperature distributions of n-heptane flames for  $V = 20$  cm/s and  $\Omega_O = 13\%$ - $21\%$ .

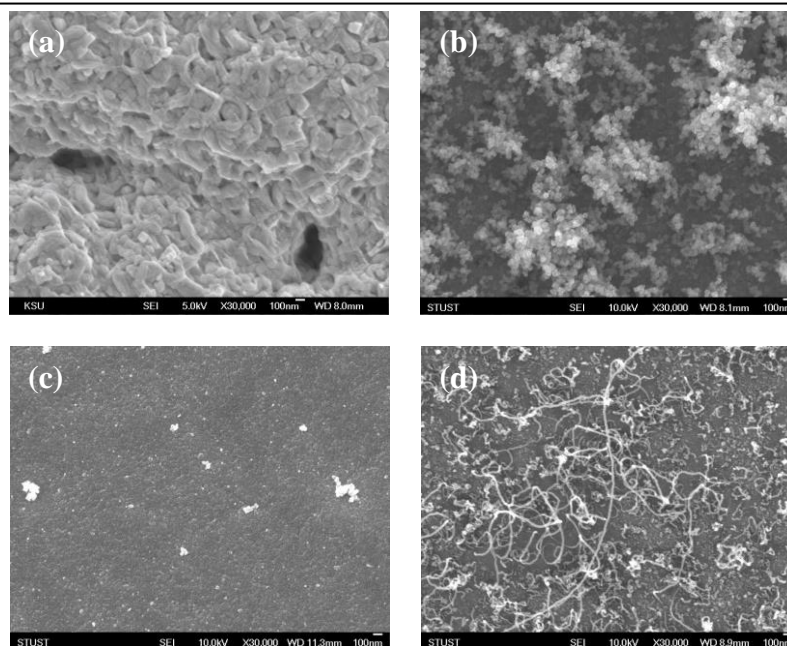


Figure 5. SEM images of grid surfaces (30000x) at  $V = 20$  cm/s and sampling position 1.5 mm below the blue flame. (a):  $\Omega_O = 21\%$ . (b):  $\Omega_O = 19\%$ . (c):  $\Omega_O = 17\%$ . (d):  $\Omega_O = 15\%$ .

## References

- [1] Kroto HW, Heath JR, O'Brien SC, Curl RF, Smalley RE. (1985). C60: Buckminsterfullerene. *Nature*. 318: 162.
- [2] Iijima S. (1991). Helical microtubules of graphitic carbon. *Nature*. 354: 56.
- [3] Novoselov KS, Geim AK, Morozov SV, Jiang D, Zhang Y, Dubonos SV, Grigorieva IV, Firsov AA. (2004). Electric field effect in atomically thin carbon films. *Science*. 306: 666.
- [4] Yuan L, Saito K, Pan C, Williams FA, Gordon AS. (2001). Nanotubes from methane flames. *Chem Phys Lett*. 340: 237.
- [5] Unrau CJ, Axelbaum RL, Fraundorf P. (2010). Single-walled carbon nanotube formation on iron oxide catalysts in diffusion flames. *J Nanopart Res*. 12: 2125.
- [6] Li Z, Zhu H, Xie D, Wang K, Cao A, Wei J, Li X, Fan L, Wu D. (2011). Flame synthesis of few-layered graphene/graphite films. *Chem Commun*. 47: 3520.
- [7] Liu Y, Pan C, Wang J. (2004). Raman spectra of carbon nanotubes and nanofibers prepared by ethanol flames. *J Mater Sci*. 39: 1091.
- [8] Hall B, Zhuo C, Levendis YA, Richter H. (2011). Influence of the fuel structure on the flame synthesis of carbon nanomaterials. *Carbon*. 49: 3412.
- [9] Hou SS, Lin TH. (1993). A liquid-pool simulation of droplet combustion in a swirl flow. *J Energ Resour Technol*. 115: 175.